

Advance Warning of Loop Current from Single-Site SeaSonde on Genesis Oil Platform in the Gulf of Mexico

D. Barrick, R. Long, C. Whelan
CODAR Ocean Sensors
1914 Plymouth Street
Mountain View, CA 94043, USA
Don@CodarOS.com

C. Cooper, J. Abadin
Energy Technology Company
ChevronTexaco
San Ramon, CA 94583
CortCooper@ChevronTexaco.com

Abstract – A single SeaSonde HF radar operates on Chevron's Genesis deep-water floating platform in the Gulf of Mexico. The radar's purpose is to provide advance warning of strong loops or eddies that approach the rig. A single radar like this, however, only produces a map of the surface current component toward or away from the radar, called a radial map. A pair of radars with overlapping coverage is required for a 2D total vector map.

Despite this limitation, and overcoming the strong antenna pattern distortions caused by the all-steel rig, useful information was obtained to a distance of 90 km. To verify the accuracy and utility, comparisons were done with an ADCP 72 km away. Low-pass filtering was used to remove short-term inertial oscillations, revealing close agreement with the 40-m deep ADCP measurement of the persistent geostrophic loops. Both saw the strong loop features.

I. INTRODUCTION

HF coastal radars [1], from which the SeaSonde evolved 13 years ago, are now an accepted technology for surface current mapping from the coast. More than 150 SeaSondes operate worldwide, most in real time. Normally two or more radars view a common area, and from the 1D radial velocities that each radar measures, a map of 2D horizontal velocity vectors is synthesized.

Because CODAR employs a compact antenna system in contrast with the classic long phased arrays used historically at HF, operation from an offshore oil platform is possible and began over 20 years ago. Joint industry projects between Gulf Oil (later merged with Chevron) and Saga Petroleum were conducted with an older CODAR unit in the North Sea from 1983-1987 [2]. These demonstrated the feasibility of radial current mapping and directional wavefield measurements. Wave-induced motions of floating platforms were found not to adversely affect current mapping from the first-order Bragg echoes.

Two major drawbacks have impeded the acceptance of SeaSonde systems up to now for operational use on offshore platforms. The first has been the strong distortion of antenna patterns by the inescapable, ubiquitous metal of the rig. This impacts accurate determination of echo bearing unless calibration methods can be applied. This issue has been mitigated recently by measuring the pattern using a boat-transported transponder unit. A second drawback has been real-time communication with the radar computer for data access and system support. The recent availability of Internet for broadband communication and control has mitigated the latter drawback.

Operation of two radars as a pair from offshore rigs -- to provide overlapping radial coverage so that 2D vector maps can be produced -- is not realistic. The primary rationale for location is oil/gas recovery, and this cannot be compromised.

The next section discusses the issue of antenna pattern distortion, partial coverage over 360°, and how we deal with these issues. The last section shows comparisons with independent ADCP comparisons, demonstrating the ability of radial surface current measurements to reveal the desired deeper loop features after low-pass filtering to remove short-term noise-like inertial oscillations that dominate in the upper water column. Agreement is very good.

II. DEALING WITH ANTENNA PATTERN DISTORTION

A. Bearing Determination in HF Radars

Three quantities are observed by an HF radar: range to target (from echo time delay), target radial velocity (from Doppler), and target bearing. The first two are obtained in a straightforward manner, and cause no significant error for in current mapping. Incorrectly determining bearing is therefore the source of all bias errors, as distinguished from zero-mean random errors due to noise.

HF radars operate at three orders of magnitude lower frequency than their much more common microwave cousins. Thus the radar wavelength at HF is tens of meters, contrasted with a centimeter or two at microwave. This impacts antenna design and their sizes.

If one resorts to conventional radar technology to form and scan a narrow beam -- as microwave radars do -- the antenna aperture must be many wavelengths (10-50) in extent. At microwave, this is done with a parabolic dish that may be 1 m in diameter, a relatively compact unit. Extending this by three orders of magnitude to HF, the antenna size to form an equivalently narrow beam becomes 1 km. This is far too large to rotate mechanically. Arrays of elements that are phased together over this linear span -- called a phased array -- are the equivalent. Such arrays were built in the early days of HF radar, but their cost and size impeded their utility and practical application.

Because of these antenna size issues and the need to observe and map currents over large angular sectors (up to 360° from a rig), all HF radars operate in the following mode. The transmit antenna "floodlights" the desired sector simultaneously. Hence it has a requirement for minimal directive properties. All target bearing information is obtained with the receiving antenna: either a large phased array that forms and scans beams, or the compact CODAR direction-finding antenna.

CODAR is a concept developed 33 years ago by the first author to obviate the disadvantages of the large phased-array systems. The present CODAR version, called the SeaSonde[®], employs two crossed loops and an omni-directional monopole for the receive system. Housed in a compact box on a post, signals from the three elements determine the direction of targets or sea echo.

B. Antenna Placement on Genesis and Offshore Rigs

One always seeks an ideal location for the HF antennas, with an unimpeded field of view over 360°, and away from vertical structures so as to minimize distortion to the receive antenna pattern. Such a location might be at the top of the derrick, the highest point on the rig. Because of operational constraints (e.g., helicopter deck and takeoff/landing flight hazard), compromises result in reduced performance for the radar. The transmit antenna installed for 13 MHz is a 5-m whip (monopole), and the receive unit is a small box on a 3-m post. The derrick was removed so it was not available. The smaller receive antenna was located near the flight deck. The transmit antenna had to be put down low, so that blockage in some sector was inevitable. Since the expected loop and eddy currents are always seen in the Southern half-space, the transmit vertical whip was placed below the level of the upper deck on the South side. Indeed, this resulted in weaker signals to the North that gave unreliable radial vectors, and so this sector is ignored. This is seen in a typical radial vector map such as that of Fig. 1.

C. Antenna Pattern Distortion and Its Effects

Loop receive antennas should have cosine patterns vs bearing angle on the horizon, and the monopole should be omnidirectional, according to textbook theory. In practice, however, the patterns -- though perfect when they leave the factory-- are distorted by metallic objects in the near field (within a wavelength), including the very cables running to the antenna unit. The inevitable nearby metal everywhere on an offshore rig constitutes a formidable challenge that is impossible to avoid [3]. Proper location -- guided by real-time boat-borne transponder measurements -- can produce patterns to serve as calibration that remove most of the biases. These patterns are taken with the boat circling the rig a few hundred meters away, generally completed within an hour. An example is shown in Fig. 1 (overlain on a radial current vector map), where the two measured loop patterns are normalized by dividing by the monopole pattern at each angle. The curves show only the amplitude (absolute value); the pattern phase is equally important for bearing determination but we omit showing it here. The big red and blue arrows in the center show the expected positions of the peaks and nulls of the patterns, if they were ideal. Clearly, the distortion from "ideal" is significant, as the resemblance to sine and cosine is barely recognizable.

D. MUSIC Bearing Determination with Distorted Patterns

With CODAR direction finding (DF), one uses the complex normalized voltage patterns of the two antennas to determine signal bearing. If the patterns were perfect sine/cosine shapes, the simplest DF algorithm could be a simple arc-tangent function of the loop voltage ratios. In practice, it is possible to resolve two bearings for the same target over signal, but the simple arc-tangent algorithm cannot be used for DF in this more complex case. Furthermore, a distorted pattern negates any attempt to apply a tangent-related rule. We have found that the most robust DF algorithm to handle these complexities is MUSIC, coined by Schmidt [4]. This has been used with CODAR SeaSondes for current mapping with considerable success over the past decade [5]. See [6] for a readable synopsis of this method for CODAR.

In the application of MUSIC, the algorithm requires antenna responses, i.e., patterns measured with the transponder. When this is done, we find that the bearing biases to the radial current maps are removed, but at the expense of some bearing gaps in the retrieved radial velocity maps. Solutions are found less frequently in certain angle sectors when patterns are distorted so they have multiple values. This gappiness is evident in Fig. 1.

III. GENESIS SEASONDE RESULTS AND COMPARISONS

A. Radial Velocity Maps at 13 MHz

The Chevron Genesis oil platform in the Gulf of Mexico is located at coordinates: 27° 45' N; 90° 31' W. Water depth at the platform is 900 m, and the distance from the nearest land at Southwest Pass in Mississippi is 168 km. Maximum range of the radar varies between 60 and 90 km, depending on environmental conditions (external noise/interference as well as sea state). We chose to operate with a 6 km range cell (twice the size of the normal 3 km cell used at 13 MHz) so as to optimize range at slight expense of spatial resolution. Fig. 1 is a typical example of a radial vector map produced hourly. As stated earlier, the coverage in the North sector is sparse and unreliable because of the antenna radiation blockage in that direction by the bulk of the rig; all data in that sector therefore is being ignored.

During a trial period after installation from July 15 – October 20, 2004 the SeaSonde produced hourly radial current maps. Oceanographic specialists monitored these maps during this period. One particularly energetic loop current feature moved into the radar coverage for a time. This was confirmed by other sources, and comparisons are discussed below. Ascertaining the intensity of advancing features such as this at a distance eliminates the necessity of sending a survey vessel out into the area to obtain these measurements, which is a costly endeavor.

The SeaSonde radial map data now are being observed daily by Chevron staff, both metocean specialists and rig operating personnel. Other information about loop current flows are available, but over limited spatial and temporal scales. For example, satellite altimetric sea-surface height provides estimates of geostrophic flow, but days after the fact. Sea surface temperature from orbiting infrared remote sensors observe large scale feature movement, but the Gulf of Mexico is obscured by clouds a large percentage of time. Sporadic drifter measurements augment these other sources. Finally, NRL at Stennis Space Center [http://www7320.nrlssc.navy.mil/IASNFS_WWW/] runs a numerical model that estimates large-scale flow and temperature in real time, but real-time observations still constitute the preferred source of information. The SeaSonde radial maps such as that in Fig. 1, for example, reveal the onset of strong currents to the SE, which in fact constitutes the advance of an intruding loop feature that is confirmed by the NRL model.

B. Data Validation Using ADCP on Atlantis Platform

Radial maps like that shown in Fig. 1 are doubly difficult to interpret. Firstly, it takes interpretative skill to visualize the radial features one should expect from a 2D picture of loop current flow patterns; or conversely, to look at a radial map and relate it to an underlying loop pattern. Secondly, surface currents include not only the desired, slowly moving geostrophic loop/eddy flow, but also noise-like surface variations whose time and space scales are smaller than the loop. Valid questions to be answered are: (1) Are there effective ways to remove the small-scale fluctuations in the surface currents that obscure the large-scale loop features? (2) After low-pass filtering, how well can the SeaSonde radial velocities at the surface represent the deep-water geostrophic flows that are of interest?

We employ acoustic Doppler current profiler (ADCP) data from the Atlantis platform. At coordinates 27° 15'N; 90° W, this rig is 72 km to the SE, in the region where the onset of intruding loop features are expected. Its position is marked on Fig. 1. The ADCP is mounted on the platform leg, with the closest bin being 40 m below the surface. Thus only features that penetrate from the surface to depths past 40 m will be seen by both sensors. Geostrophic loops and eddies fall into this category.

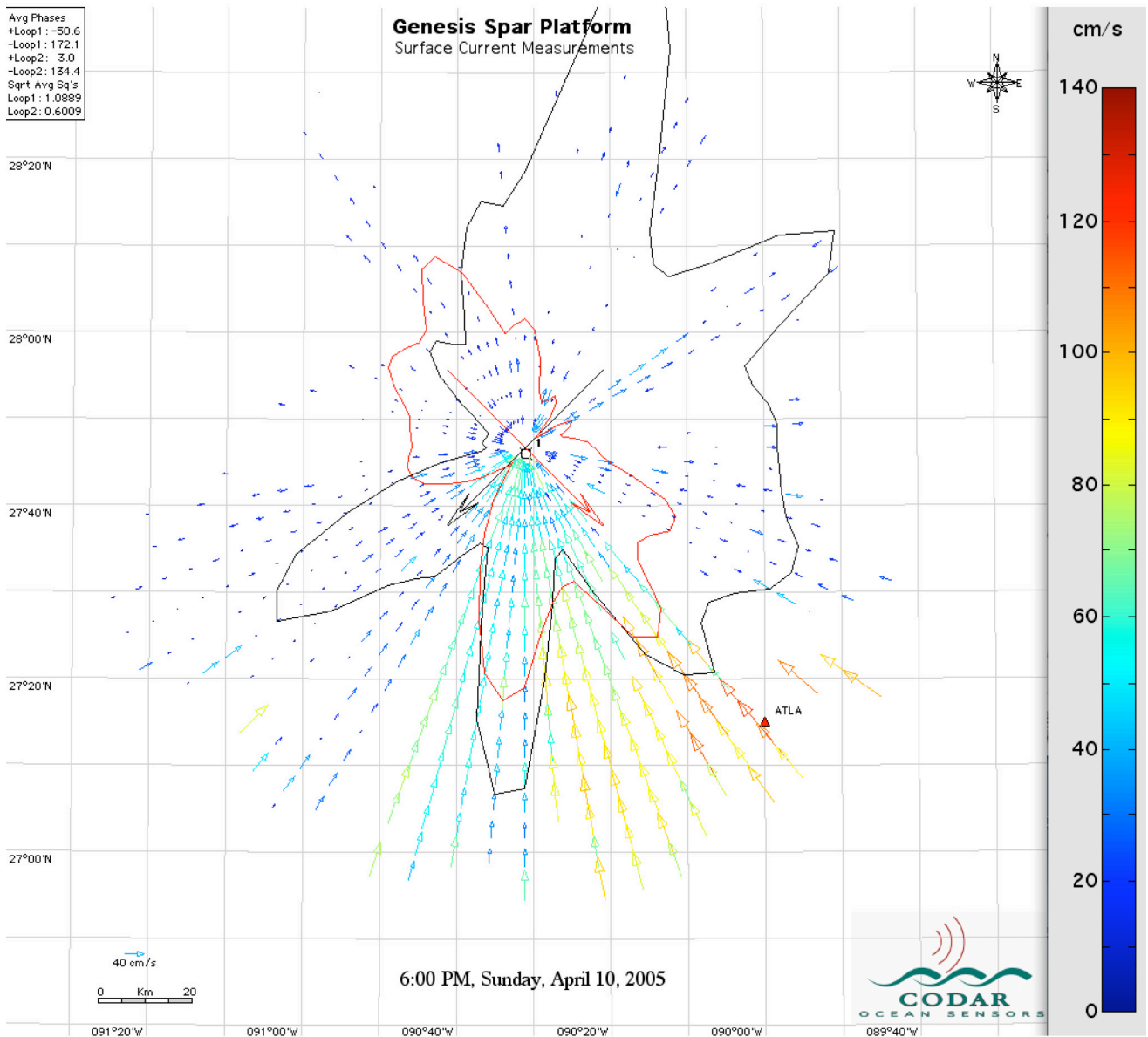


Fig. 1. Typical radial current velocity map measured at Chevron Genesis oil platform in Gulf of Mexico. Strong loop feature to SE is seen in the data. Radial currents in North sector are unreliable because of blockage of antenna radiation by the rig. Receive antenna normalized amplitude patterns for the crossed loops are shown as black and red curves; large black and red vectors from center denote expected directions of maxima and minima of idealized cosine patterns. Red triangle to SE is location of ADCP on Atlantis rig that was used for data comparisons with the radar data.

C. Data Filtering and Comparisons

In order to allow a meaningful comparison of SeaSonde data at the Atlantis position 72 km to the SE, the ADCP time series at its 40-m deep bin was resolved into the component pointing toward and away from the radar. Both sets of data were registered to hourly intervals, from July 15 – October 20, 2004. Raw hourly radial data from the SeaSonde at Atlantis are shown in Fig. 2. Units of the horizontal axis are days after July 15, 2004 at 00:00. Hence 100 days corresponds to October 20. Gaps are shown where either system obtained no data. History displays such as this are useful in observing trends over time.

The raw hourly data are plotted as the green curve for both SeaSonde and ADCP. The short-term "noise" is inertial oscillations for the most part, with the inertial period being ~26 hours at the Genesis latitude. Some diurnal "sea breeze" pulsing is aliased into this near-daily noise. Tidal contributions are negligible in this part of the Gulf of Mexico. These fluctuations are obviously greater at the surface for CODAR than at the 40-m depth of the Atlantis ADCP, although they are unmistakably

present there also. A trend beneath the fluctuations is evident, but low-pass filtering represented by the red curves reveals both the long-term geostrophic flows and the constancy of these flow features with depth.

The low-pass filtering we did used a time constant of 52 hours (~2 days), twice the inertial period. This was done to remove both the diurnal, inertial, as well as short-term weather effects like storms and fronts that pass by. We employed a rule that requires 25% of the points in a 52-hour sliding window to be present. If this condition is met, a mean is calculated for the center of that sliding window every hour. If less than 25% are present in the sliding window, then a gap is left at that point. Therefore, some of the short-term gaps in the hourly raw data are filled in, but the longer ones remain.

Statistics behind the plots are: raw RMS difference between 881 common points is 25 cm/s and correlation coefficient is 0.63; filtered RMS difference between 1578 common points is 14 cm/s and correlation coefficient is 0.87.

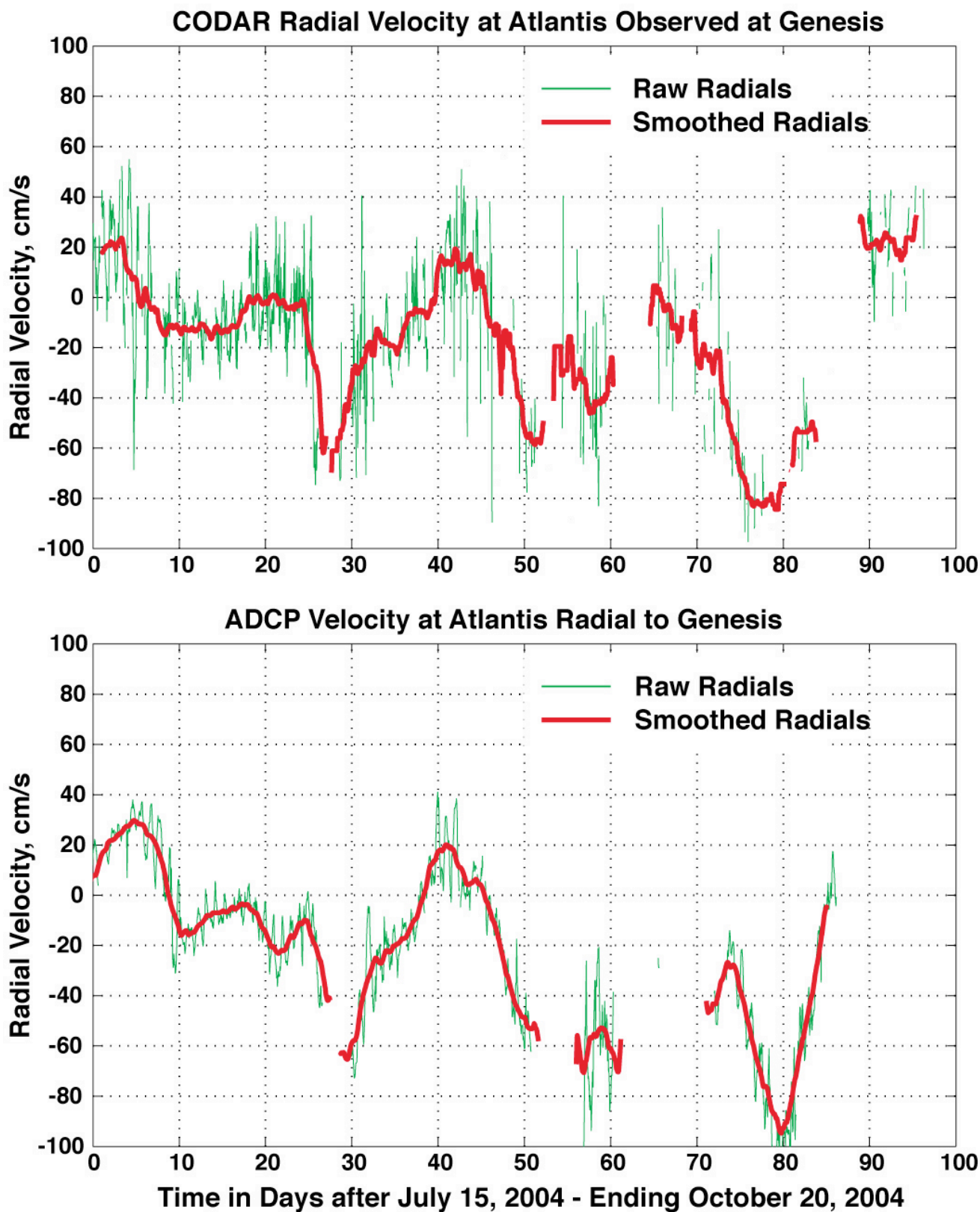


Fig. 2. CODAR SeaSonde radial velocity at top vs. time in days after July 15, 2004, calculated at location of Atlantis rig 72 km to SE; at bottom is the component of ADCP velocity radially directed toward Genesis radar measured 40-m below the surface at Atlantis (the uppermost measurement available). Data for both are plotted hourly; no data were available in gap regions. Green curves are raw radial data values every hour. Red curve is output from a 52-hour low-pass filter of raw hourly data. The low-pass filtering removes diurnal fluctuations, inertial oscillations, and short-term weather influences near surface, revealing agreement of deeper geostrophic loop and eddy features.

IV. SUMMARY AND FUTURE PLANS

By low-pass filtering radial SeaSonde surface current data to remove short-term fluctuations, we have shown that a single radar indeed reveals desired deeper geostrophic loop and eddy features at a sufficient distance from an oil platform to allow useful operational planning. Correlation between surface measurements by the radar and flows 40-m deep is 87%. These comparisons were done at a distance of 72 km from the radar.

Because radial velocity map features are difficult to interpret in terms of the 2D circulation pattern, two improvements are planned for the future: (1) Filtered colorized map movie loops over weekly periods will be displayed, allowing the viewer to focus on strong features as they migrate into the region near the platform. (2) Total-vector map estimates with larger scale resolution will be constructed using the Navier-Stokes equations as a constraint to produce the unknown azimuthal velocity component from the radial components measured by the radar. The latter is akin to the methodology that allows geostrophic circulation to be constructed from satellite altimetric measurement of sea-surface topographic slope.

REFERENCES

- [1] D. Barrick, M. Evans, and B. Weber, "Ocean surface currents mapped by radar," *Science*, vol. 198, pp. 138-144, 1977.
- [2] B. Lipa, D. Barrick, J. Isaacson, and P. Lilleboe, "CODAR wave measurements from a North Sea semisubmersible", *IEEE J. Oceanic Engr.*, vol. OE-15, pp. 119-125, 1990.
- [3] D. Barrick and B. Lipa, "Correcting for distorted antenna patterns in CODAR ocean surface measurements," *IEEE J. Oceanic Engr.*, vol. OE-11, pp. 304-309, 1986.
- [4] R. Schmidt, "Multiple emitter location and signal parameter estimation," *IEEE Trans. on Antennas and Propagation*, vol. AP-34, pp. 278-280, 1986.
- [5] D. Barrick and B. Lipa, "Radar angle determination with MUSIC direction finding," U. S. Patent No. 5,990,384, 1999.
- [6] D. Barrick and B. Lipa, "Evolution of bearing determination in HF current mapping radars," *Oceanography*, vol. 10, no. 2, pp. 72-75, 1997.

© Copyright 2005 IEEE